s-d bands of liquid La

L. E. Ballentine
Department of Physics and Theoretical Science Institute, Simon Fraser University, Burnaby, British Columbia, Canada, V5A 1S6
(Received 5 October 1981)

The electronic structure of liquid La is calculated by applying the linear combination of atomic orbitals method to a cluster of 365 atoms. Although the *s* and *d* bands are of nearly the same width and are strongly hybridized in the solid, we find that in the liquid the *s* states retain their propagating character much more so than do the *d* states. This suggests, tentatively, that in the calculation of the conductivity it is more nearly correct to treat only the *s* electrons as current carriers than to regard both *s* and *d* electrons as conduction electrons.

I. INTRODUCTION

The electronic structure of lanthanum is interesting for several reasons. The *s* and *d* valence bands are of nearly the same width and occupy nearly the same energy range. Thus it is necessary to treat them on an equal basis, in contrast to the iron series transition metals in which the *s* bands are weakly bound while the *d* bands are tightly bound.

The Hall coefficient is positive for both solid and liquid La. Now the Fermi surface is dominated, over at least some neighborhood of the {100} directions, by an inverted (holelike) *d* band (see Fig. 1). This raises the question of whether the sign of the Hall effect might be due to the survival of this band upon melting.

Calculations of the electrical resistivity of liquid transition[1] and rare-earth metals[2] have often been based on the assumption that the *s* electrons, but not the *d* electrons, are the effective current carriers. This assumption has been criticized. Clearly it has no *a priori* plausibility when the *s* and *d* bands are nearly coextensive, as is the case for La, but a calculation of the electronic states in the liquid phase is necessary to resolve the issue.

For these reasons we present a linear combination of atomic orbitals (LCAO) calculation for a cluster that simulates a sample of liquid La. The model includes only the *s* and *d* valence bands. The narrow unoccupied *f* band is omitted from the model because it is sufficiently far above the Fermi energy to have no effect on electronic transport.

Section II describes the version of the LCAO method that we use, and it is tested in Sec. III by calculating the band structure of fcc La. Sections IV, V, and VI describe the construction of atomic clusters to simulate the liquid state, and the calculation of their electronic structure. Finally the conclusions are summarized in Sec. VII.

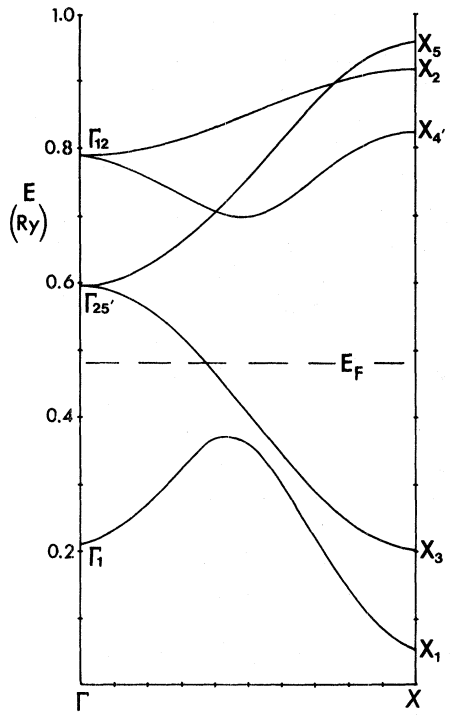

FIG. 1. *s* and *d* bands for fcc La along the [100] direction. The point *X* is a distance $2\pi/a = 0.6276$ a.u. from the zone center (Γ). Lengths are in atomic units (Bohr radii) and energies are in Rydbergs. The narrow *f* band at about 0.7 Ry is omitted from the model.

II. LCAO METHOD

A. Overlap of basis functions

In this application of the LCAO method, we express all wave functions and potentials as linear combinations of Slater-type basis functions of the form

$$f^n_{lm}(\alpha,\vec{r})=e^{-\alpha r}r^{n+l-1}Y^m_l(\hat{r}) . \tag{1}$$

Thus the first problem is the computation of the overlap integral for two such functions centered on different atoms. Although several of these integrals have been evaluated in the past, they are scattered throughout the literature in various notations and often expressed in an inconvenient coordinate system. For this reason, as well as the possibility of errors in published formulas, we have chosen to generate all the overlap integrals in a systematic fashion that is most convenient for computation.

An integral of the form $(f_1(\vec{r}),f_2(\vec{r}-\vec{R}))$ is a convolution, hence its Fourier transform is the product of the Fourier transforms of $f_1(\vec{r})$ and $f_2(\vec{r})$. [Here $f_1(\vec{r})$ denotes $f^{n_1}_{l_1m_1}(\alpha_1,\vec{r})$.] These can readily be obtained for the case $n_1=n_2=0$. The inverse Fourier transform can be evaluated by contour integration, and the overlap integrals for n_1 and $n_2>0$ can be generated by differentiation with respect to α_1 and α_2.

Though simple in principle, this calculation is too tedious to carry out by hand for any but the simplest cases. However, the necessary evaluation of the residues at high-order poles, differentiation to generate values of n_1 and $n_2>0$, and the use of l'Hospital's rule to obtain the limit $\alpha_1=\alpha_2$ were conveniently performed analytically by means of a program written in the symbolic computing language FORMAC73. The resulting formulas for $(f_1(\vec{r}),f_2(\vec{r}-\vec{R}))$ as functions of α_1,α_2, and $\vec{R}$, which are too lengthy to reproduce here, are automatically expressed in FORTRAN notation and may be compiled for numerical evaluation.

B. The eigenvalue equation

The eigenvalue equation

$$H\,|\psi\rangle=E\,|\psi\rangle \tag{2}$$

is transformed into a matrix equation by expanding in a suitable set of atomic orbitals,

$$|\psi\rangle=\sum_i c^i\,|\phi_i\rangle , \tag{3}$$

whence (2) yields

$$\sum_j H^i{}_j c^j=Ec^i \tag{4}$$

with

$$H^i{}_j=\sum_k (S^{-1})_{ik}H_{kj},\quad S_{ij}=\langle\phi_i\,|\,\phi_j\rangle ,$$

and

$$H_{ij}=\langle\phi_i\,|\,H\,|\,\phi_j\rangle .$$

The raised and lowered indices emphasize the analogy with covariant and contravariant components in geometry, a distinction that is necessary whenever the overlap matrix S_{ij} is not diagonal.

An important advance in the theory was made by Anderson,[3] who showed that the "best" atomic-like orbitals for describing a band of eigenfunctions of the Hamiltonian

$$H=T+\sum_a V_a , \tag{5a}$$

where V_a is the potential centered on atom a, are determined by the equation

$$\left[T+V_a+\sum_{b\neq a}V^{\rm ps}_b\right]|\phi_i\rangle=\epsilon_i\,|\phi_i\rangle . \tag{5b}$$

The effects of all atoms except a are contained in pseudopotentials of the form

$$V^{\rm ps}_b=\left[1-\sum_\beta |\phi_\beta\rangle\langle\phi_\beta|\right]V_b ,$$

which is weaker than the atomic potential because the projection onto the orbitals on atom b has been subtracted.

It can be shown from (5b) that

$$H^i{}_j=\langle\phi_i\,|\,V_i\,|\,\phi_j\rangle \tag{6}$$

for orbitals i and j centered on different atoms, and $H^i{}_j=\delta_{ij}\epsilon_i$ when i and j are on the same atom. In spite of appearances, (6) does not neglect the nonorthogonality of orbitals on different atoms. By means of a numerical example, Anderson showed that although the perturbation of $|\phi_i\rangle$ by the pseudopotential term in (5b) is not negligible, nevertheless it is sufficient for the evaluation of (6) to approximate $|\phi_i\rangle$ by atomic orbitals that are simply eigenfunctions of $T+V_a$.

C. Exchange and correlation effects

Although the total potential can always be written formally as a sum of contributions centered on

each atom as in (5a), one may not merely superimpose free atom potentials to obtain the total. This is so even if the total electron density is given by the sum of atomic electron densities, because the exchange-correlation potential is not linear in electron density. The Hohenberg-Kohn-Sham[4] modification of the Slater exchange potential,

$$V_x(\vec{r}) = -\alpha_x e^2 \tfrac{3}{2} \left[\frac{3}{\pi} \rho(\vec{r}) \right]^{1/3}, \tag{7}$$

where $\rho(\vec{r})$ is the electron density, e is the electron charge, and $\alpha_x = \frac{2}{3}$ has been used to compute self-consistent orbitals for a single atom. In calculating the overlap of this atom with a similar neighboring atom at relative position $\vec{R}$, the sum of the atomic potentials must be corrected for nonadditivity of V_x by adding the term

$$\delta V_x(\vec{r}) = -c\{ [\rho(\vec{r}) + \rho(\vec{r}-\vec{R})]^{1/3} - [\rho(\vec{r})]^{1/3} - [\rho(\vec{r}-\vec{R})]^{1/3} \}. \tag{8}$$

The value of the constant c is implicit in (7).

The transfer matrix element (6) should now be computed as

$$H^i{}_j = \langle \phi_i \mid V_i^{(0)} \mid \phi_j \rangle + \langle \phi_i \mid \delta V_x \mid \phi_j \rangle \tag{9}$$

where $V_i^{(0)}$ is the free atom potential on the same center as ϕ_i. The second term partially cancels the first, and incidentally explains why Bromley *et al.*[5] found it necessary to apply an *ad hoc* reduction factor to their two-center integrals, which were just the first term of (9).

The second term of (9) does not have the form of a two-center integral and so it is difficult to compute. But fortunately, $\delta V_x(\vec{r})$ is slowly varying (see Fig. 2), and it may reasonably be approximated by a constant over the region of overlap of the neighboring orbitals.

III. BAND-STRUCTURE CALCULATION

In order to test the method, the band structure of fcc La was computed. Self-consistent atomic orbitals were obtained, using (7) to approximate exchange effects, and the transfer matrix elements (9) were then computed. But since the objective is not primarily to study crystal band structure, but rather to obtain realistic LCAO parameters for application to the liquid state, two adjustable parameters were used. The difference between the s and d atomic levels was adjusted to yield the correct separation between s and d bands at the zone

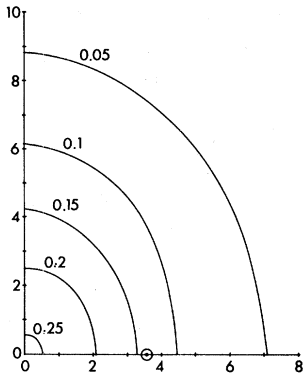

FIG. 2. Contours of $\delta V_x(\vec{r})$ (Ry), the nonadditive part of the potential of two atoms. One atom is shown on the $+x$ axis, the other being the same distance from the origin along the $-x$ axis.

center, and the constant δV_x was adjusted to yield the correct s band width ($X_{4'} - \Gamma_1$), as earlier computed by Glotzel and Fritsche.[6] The value so obtained, 0.176 Ry, is apparently consistent with an average of $\delta V_x(\vec{r})$ over the bonding region. The same value yields a good shape and width for the d bands in the [100], [110], and [111] directions. The only significant difference between our band structure (Fig. 1) and that of Glotzel and Fritsche is the depression of the lowest two bands at X in our results. Indeed, our results for zero pressure resemble their results at elevated pressure as far as this feature is concerned. However, since the qualitative features of the band structure that are relevant to this work (see Introduction) are present at both high and low pressure, we shall not concern ourselves further with the comparative accuracies of our band-structure calculation and those of others.

IV. SIMULATION OF THE LIQUID

A cluster of 365 atoms, representing a sample of liquid La, was generated by the Monte Carlo method, using as the interatomic potential

$$\phi(r) = \begin{cases} c(X^{-6} - X^{-4}) + H, & X < 2 \\ 0, & X \geq 2 \end{cases} \tag{10}$$

with $X = r/r_0$, $r_0 = 5.669$ a.u., $c = 1.0$ eV, $H = 0.0469$ eV. This form was suggested by inversion of the hypernetted-chain (HNC) equation[7] to obtain $\phi(r)$ from the measured structure factor,[8] but the scale parameter r_0 was empirically adjusted since the inversion of the HNC equation is known

to systematically overestimate the radius of the repulsive core. The cluster is in a cubic volume, surrounded by periodic replicas of itself to avoid surface effects.

The simulation was performed for a temperature 1243 K, slightly above the melting point, from a fcc lattice as the initial configuration. Three criteria were used to determine the reaching of equilibrium:

(a) The fluctuations in energy no longer have any systematic component.

(b) The pair-distribution function reached a stable limit that does not exhibit peaks characteristic of the crystal.

(c) Slices of the cluster were examined graphically to see whether the atoms still tended to lie in lines parallel to the initial crystal axes.

These three criteria are successively more difficult to satisfy.

The first and second criteria were satisfied after 150 iterations of the Monte Carlo program (that is, each of the 365 particles attempted to move 150 times). The model pair distribution $g(r)$ was in reasonable overall agreement with experiment, but the first peak was somewhat too sharp. A further 100 iterations were performed for a temperature 17% higher, equivalent to reducing the strength of $\Phi(r)$, yielding the pair distribution shown in Fig. 3, for which the third criterion is also well satisfied. The remaining discrepancy between the model $g(r)$ and experiment is due to the repulsive core of our potential (10) being somewhat too hard. The results for electronic structure should not be seriously affected by this detail.

The electronic structure calculations were performed on clusters with free surfaces (the periodic replication being used only during the generation of the clusters). The results for the cluster which was produced by 150 iterations [for which criterion (c) was not quite satisfied] did not differ significantly from those (Figs. 4 and 6–8) for the final cluster. This confirms that our clusters are adequately representative of the liquid state, even though 250 iterations of the Monte Carlo program are a rather small amount for a simulation.

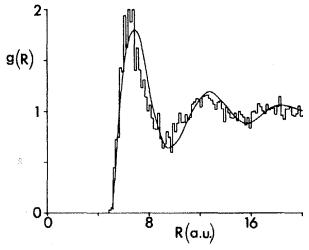

FIG. 3. Radial distribution function for liquid La near the melting point, according to experiment (Ref. 8) (smooth curve) and as simulated in a cluster of 365 atoms (histogram).

V. THE RECURSION METHOD

The theory and applications of the recursion method have recently been reviewed.[9] By repeated application of the equation

$$H\,|\,u_n\rangle = a_n\,|\,u_n\rangle + b_{n+1}\,|\,u_{n+1}\rangle + b_n\,|\,u_{n-1}\rangle$$

one generates a chain of functions which form the basis of a tridiagonal representation of H. For the nonsymmetric matrix (9), we used the two-sided recurrence method,[10] in which the above equation is supplemented by a similar one for $H^\dagger$. The tridiagonal form for H leads directly to a continued fraction representation of the Green's function,

$$G_u(E) = \langle u\,|\,(E-H)^{-1}\,|\,u\rangle\ , \tag{11}$$

where $|\,u\rangle = |\,u_0\rangle$ is the arbitrary initial vector chosen to begin the recursion. The imaginary part of the Green's function yields the projected density of states on the vector $|\,u\rangle$,

$$\begin{aligned} n_u(E) &= \lim_{\epsilon\to 0} -\frac{1}{\pi}\mathrm{Im}G_u(E+i\epsilon) \\ &= \sum_n \langle u\,|\,\psi_n\rangle\delta(E-E_n)\ . \end{aligned} \tag{12}$$

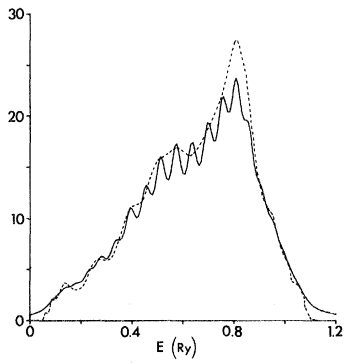

FIG. 4. Local density of states on a central atom in the liquid cluster by the following two methods: solid curve, Eq. (12) with imaginary part $\epsilon=0.03$ added to the energy, and dashed curve, Cambridge subroutine RECTAB, which differentiates an approximation to the cumulative distribution. The units of state densities are electron states per Ry atom in Figs. 4–8.

Here $|\psi_n\rangle$ and E_n are the true eigenvectors and eigenvalues of the Hamiltonian. It has been common to take $|u\rangle$ to be a localized orbital on some atom, in which case (12) is called the local density of states (DOS). We shall sometimes take $|u\rangle$ to be an extended wave function in order to investigate the propagating character of the states. The projected density of states onto a multidimensional subspace is obtained by summing the projected densities on an orthogonal set of vectors that spans the subspace.

In practice, the Green's function is computed for a finite cluster of atoms and the continued fraction is truncated at some finite level. Either of these truncations causes the density (12) to be strictly a set of delta functions. There are two practical methods for obtaining a smoothed spectrum. The first is to keep the imaginary part of the energy in (12) nonzero and at least as large as the spacing between delta functions. This method is always applicable, but it may obscure detail and it replaces band edges with Lorentzian tails. The second method is based on differentiation of the mean of upper and lower bounds to the cumulative distribution. It is implemented in subroutine RECTAB of the Cambridge Recursion Library.[11] It yields apparently superior results in many cases, but is sometimes unusable because it can preserve some unbroadened delta functions. The two methods are compared in Fig. 4. The oscillations in the first case are associated with the truncation of the continued fraction, and have no physical significance. Figures 6–8, for the liquid state, were made by the second method; however, for a crystal (Fig. 5), only the first method gave a reasonable result. A third method, extending the continued fraction to infinite order by means of an estimated asymptotic form of the coefficients, was found to be ineffective.

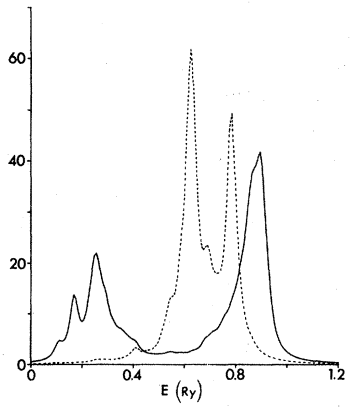

FIG. 5. d state spectra for a crystal cluster for $\vec{k}=(0,0,0)$ (dashed curve) and $\vec{k}=(0,0,0.5021$ a.u.) (solid curve), with $\epsilon=0.02$ Ry. Small deviations of the peak positions from the bands of Fig. 1 are due to the finite size of the cluster.

From the peaks of the projected densities of states onto the Bloch-like vectors,

$$|u\rangle=\sum_j e^{i\vec{k}\cdot\vec{R}_j}|\phi_j\rangle\ , \tag{13}$$

one can obtain the band structure for a crystalline cluster (Fig. 5). The sum over atoms in (13) is done for a particular (l,m) type of orbital, and the densities summed to obtain all bands corresponding to a given $\vec{k}$. The subspace spanned by wave vectors $+\vec{k}$ and $-\vec{k}$ can more easily be treated by using sin and cos instead of the complex exponentials. Each curve in Fig. 5 is the sum of ten projected densities, for sin and cos, and for $m=-2,\ldots,2$. Spurious peaks that do not correspond to any actual band may sometimes occur, however they can be distinguished from physical peaks by varying the length of the continued fraction and by varying the size of the cluster. Of course this method is impractical compared to the usual k space methods of crystal band structure computation, and it is presented only to demonstrate its effectiveness before applying it to the liquid state.

VI. RESULTS FOR LIQUID La

The Hamiltonian matrix (9) was computed from the same atomic orbitals, potentials, and fitted parameters that were determined for the crystal (Sec. III). The matrix elements for a liquid cluster were calculated as a function of the actual interatomic separations of the atoms, rather than assuming fixed values for "nearest neighbors," as has often been done. To keep the size of the matrix within reasonable bounds, all overlap integrals were cut off at a distance corresponding to second-nearest neighbors in the crystal. The clusters of 365 atoms are cubic in shape with free boundary conditions for the electronic structure calculations. All results illustrated are for the final cluster (250 Monte Carlo iterations), since the results showed no significant differences between clusters.

Figures 6 and 7 show the s and d state spectra for several values of $\vec{k}$ in (13). There is no significant dependence of the results on the orientation of $\vec{k}$ with respect to the sides of the cube. The s state spectrum exhibits well-defined peaks, although they are quite broad in the midband region where

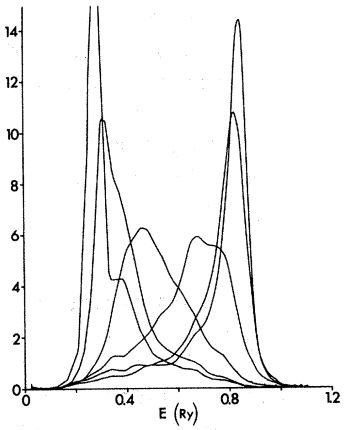

FIG. 6. s state spectra for liquid La. From left to right $k=0$, 0.1255, 0.2511, 0.3766, 0.5021, and 0.6276 (inverse Bohr radii).

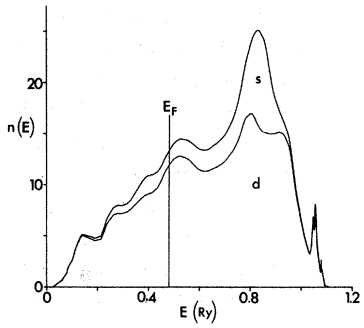

FIG. 8. Total density of electron states per atom, with s and d components shown, for liquid La. The sharp structure near the top of the band is an artifact of the imperfect smoothing routine (RECTAB).

sd hybridization is strong. The positions of the peaks yield a well-defined dispersion relation, which strongly suggests that these are propagating states. On the other hand, the d state spectrum is broad, without well-defined peaks, and exhibits very little dependence on $\vec{k}$. Indeed, all curves of Fig. 7 are quite similar to the local density of d states on one atom. Just as a flat band (E independent of $\vec{k}$) is indicative of localized atomic states in a crystal, so the $\vec{k}$ independence of these results suggest that the d states in liquid La are nearly localized. We are not claiming localization in the sense of the Anderson transition, but merely that the propagating character of the d states has been severely curtailed by the disorder.

The bulk density of states can be estimated from the local density of states on atoms away from the surface. Figure 8 shows the s, d, and total densities of states for liquid La, calculated as an average over three central atoms. There is very little variation from one atom to the other. There are 0.3 s electrons and 2.7 d electrons per atom.

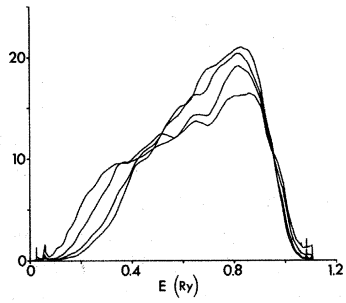

FIG. 7. d state spectra for liquid La for $k=0$, 0.1883, 0.3766, and 0.6276. As k increases, the width of the curve increases and the height decreases.

VII. CONCLUSIONS

The most striking conclusion is that in spite of the s and d bands being about equally wide and strongly hybridized in the crystal, the s band retains a clearly defined dispersion relation upon melting whereas the d band does not. The disorder is apparently more effective in disrupting the propagating character of d states than of s states.

The conjecture that the inverted d band that dominates the Fermi surface in the crystal might survive into the liquid state is not supported, so no explanation is provided for the positive Hall coefficient in liquid La.

Because s states appear to retain their propagating character in the liquid more effectively than d states, these results suggest that it is more nearly correct to regard the dc conductivity as being due to only s electrons than to regard the s and d electrons as participating equally in conduction. The tentative nature of this conclusion must be stressed, and a proper LCAO calculation of the conductivity is needed to determine the relative contributions of s and d electrons.

Note added in proof. In view of the conclusion that the propagating character of s states survives while that of d states is severely disrupted, one may wonder what would happen to p states. Using a similar model in which p states replace the d states, we find the $\vec{k}$ dependence of the p spectra to be strong but less sharply peaked than the s spectra of Fig. 6.

ACKNOWLEDGMENTS

I would like to thank Jim Hammerberg for assistance in developing some of the computer programs and Roger Haydock for useful discussions about the recursion method. This research is supported by a grant from the Natural Sciences and Engineering Research Council of Canada.

[1]O. Dreirach, R. Evans, H.-J. Güntherodt, and H.-U. Kunzi, J. Phys. F 2, 709 (1972).

[2]B. Delley and H. Beck, J. Phys. F 9, 517 (1979). On the other hand, Y. Waseda, A. Jain, and S. Tamaki, J. Phys. F 8, 125 (1978) assume that all of the 6*s* and 5*d* electrons are conduction electrons.

[3]P. W. Anderson, Phys. Rev. 181, 25 (1969). See also Sec. 10 of Bullett (Ref. 9).

[4]P. Hohenberg and W. Kohn, Phys. Rev. 136, B864 (1964); W. Kohn and L. J. Sham, Phys. Rev. 137, A1697 (1965).

[5]R. A. Bromley and R. B. Murray, J. Phys. C 5, 738 (1972); R. B. Murray, R. A. Bromley, and A. D. Yoffe, *ibid.* 5, 746 (1972); R. A. Bromley, R. B. Murray, and A. D. Yoffe, *ibid.* 5, 759 (1972).

[6]D. Glötzel and L. Fritsche, Phys. Status Solidi B 79, 85 (1977). More recent results by A. K. McMahan, H. L. Skriver, and B. Johansson, Phys. Rev. B 23, 5016 (1981) appeared when the present work was nearly complete.

[7]L. E. Ballentine and J. C. Jones, Can. J. Phys. 51, 1831 (1973).

[8]Y. Waseda, *The Structure of Non-Crystalline Materials* (McGraw-Hill, New York, 1980), Table App. 8.22.

[9]V. Heine, Solid State Phys. 35, 1 (1980); D. W. Bullett, *ibid.* 35, 129 (1980); R. Haydock, *ibid.* 35, 215 (1980); M. J. Kelly, *ibid.* 35, 295 (1980).

[10]R. Haydock and M. J. Kelly, J. Phys. C 8, L290 (1975).

[11]C. M. M. Nex, Cambridge Recursion Method Library of computer programs, available from the Secretary, T. C. M. Group, Cavendish Laboratory, Madingly Road, Cambridge, CB3 OH3, England.